Keratocyte-Derived Myofibroblasts: Functional Differences With Their Fibroblast Precursors

Ana C. Acosta,[1] Hadi Joud,[1] Mei Sun,[1] Marcel Y. Avila,[4] Curtis E. Margo,[1,3] and Edgar M. Espana[1,2]

[1]Cornea and External Disease, Department of Ophthalmology, University of South Florida, Tampa, Florida, United States
[2]Department of Molecular Pharmacology and Physiology, Morsani College of Medicine, University of South Florida, Tampa, Florida, United States
[3]Department of Pathology and Cellular Biology, Morsani College of Medicine, University of South Florida, Tampa, Florida, United States
[4]Departamento de Oftalmologia, Universidad Nacional de Colombia, Bogota, Colombia

Correspondence: Edgar M. Espana, Department of Ophthalmology, University of South Florida, Morsani College of Medicine, 13330 USF Laurel Dr., 4th floor, MDC11, Tampa, FL 33612, USA; eespana@usf.edu.

Received: January 9, 2023
Accepted: September 5, 2023
Published: October 5, 2023

Citation: Acosta AC, Joud H, Sun M, Avila MY, Margo CE, Espana EM. Keratocyte-derived myofibroblasts: Functional differences with their fibroblast precursors. *Invest Ophthalmol Vis Sci.* 2023;64(13):9. https://doi.org/10.1167/iovs.64.13.9

Purpose. In this study, we aim to elucidate functional differences between fibroblasts and myofibroblasts derived from a keratocyte lineage to better understand corneal scarring.

Methods. Corneal fibroblasts, derived from a novel triple transgenic conditional *KeraRT/tetO-Cre/mTmG* mouse strain that allows isolation and tracking of keratocyte lineage, were expanded, and transformed by exposure to transforming growth factor (TGF)-β1 to myofibroblasts. The composition and organization of a fibroblast-built matrix, deposited by fibroblasts in vitro, was analyzed and compared to the composition of an in vitro matrix built by myofibroblasts. Second harmonic generation microscopy (SHG) was used to study collagen organization in deposited matrix. Different extracellular matrix proteins, expressed by fibroblasts or myofibroblasts, were analyzed and quantified. Functional assays compared latent (TGF-β) activation, in vitro wound healing, chemotaxis, and proliferation between fibroblasts and myofibroblasts.

Results. We found significant differences in cell morphology between fibroblasts and myofibroblasts. Fibroblasts expressed and deposited significantly higher quantities of fibril forming corneal collagens I and V. In contrast, myofibroblasts expressed and deposited higher quantities of fibronectin and other non-collagenous matrix components. A significant difference in the activation of latent TGF-β activation exists between fibroblasts and myofibroblasts when measured with a functional luciferase assay. Fibroblasts and myofibroblasts differ in their morphology, extracellular matrix synthesis, and deposition, activation of latent TGF-β, and chemotaxis.

Conclusions. The differences in the expression and deposition of extracellular matrix components by fibroblasts and myofibroblasts are likely related to critical roles they play during different stages of corneal wound healing.

Keywords: stroma, keratocyte, keratocan, fibroblast, myofibroblast

Keratocytes are neural crest-derived cells that reside in the corneal stroma. They are critical in maintaining the intrinsic properties of the corneal stroma, including transparency, shape, and avascularity.[1–3] Several characteristics of the cornea contribute to its high degree of transparency: the unique hierarchical organization of its extracellular matrix, avascularity, and a precisely regulated degree of hydration. Keratocytes maintain corneal transparency by producing and remodeling extracellular matrix components, including collagens, proteoglycans, and crystallins. They are arranged between collagen lamellae and are characterized by small cell bodies with long, branching cellular processes that connect neighboring keratocytes to form an extensive network throughout the stroma.[4] The most widely recognized marker of keratocytes is keratocan, a cornea-specific proteoglycan that regulates collagen fibril thickness and spacing.[5] Other markers include aldehyde dehydrogenases 1 and 3 (ALDH1A1 and ALDH3A1), CD34, and lumican.[1,4]

Following injury, quiescent keratocytes undergo mitosis and are activated into fibroblasts that repair corneal tissue and restore function. They are characterized by loss of keratocan and CD34 expression, loss of dendritic morphology, and upregulation of vimentin expression.[6] Fibroblasts' major functions during wound healing include the production of growth factors, extracellular matrix components (collagens, proteoglycans, etc.), and matrix metalloproteinases in addition to the modulation of epithelial basement membrane regeneration and the inflammatory response.[1,6–8] In cases of extensive injury and prolonged exposure of fibroblasts to growth factors, including transforming growth factor β (TGF-β), these cells can transform into myofibroblasts. Otherwise, they undergo apoptosis.[6,9]

Myofibroblasts are commonly distinguished from other cell types by their expression of α smooth muscle actin (αSMA) and its incorporation in cytoskeletal stress fibers. They are also known to upregulate the intermediate filament proteins desmin and vimentin.[10] Myofibroblasts are defined by phenotypic features, including their contractile function, cytoskeletal organization, and dense focal adhesions.[11] Wound repair mediated by myofibroblasts is associated with larger degrees of wound contracture. Like fibroblasts, myofibroblasts synthesize extracellular matrix components, but are believed to deposit extracellular matrix in larger quantities and in a disorganized pattern, clinically causing the formation of corneal haze. Therefore, survival of myofibroblasts with uncontrolled production of matrix in a regenerating tissue contributes to excessive scar formation. In contrast, fibroblasts-mediated wound healing is less likely to lead to pathologic fibrosis [8,12] The fate of myofibroblasts after tissue repair is not entirely understood. They are believed to be cleared from the tissue by apoptosis once the influx of growth factors is attenuated, because growth factor signaling promotes myofibroblast survival. In vitro studies demonstrate that myofibroblasts may be inactivated and revert to a fibroblast-like phenotype, but this has not yet been demonstrated in vivo.[6]

Keratocytes can be induced in vitro to differentiate into fibroblasts and myofibroblasts by supplementation with growth factors, including TGF-β, platelet-derived growth factor, and fibroblast growth factor. Using standard culture conditions on plastic dishes with fetal bovine serum (FBS) supplementation, keratocytes (murine,[13] bovine,[14] rabbit,[15] primate,[16] and human[17–19]) lose their dendritic morphology and expression of keratocan and become fibroblasts resembling those in wound healing. Reliable conversion to fibroblasts is achieved with 5% FBS, and the use of much lower FBS concentrations (e.g. 0.5%) can be used to maintain and expand keratocytes in an activated state without inducing fibroblast conversion. These expanded keratocytes can then revert to quiescent keratocytes upon culture in serum-free medium.[20,21] In vitro, fibroblasts cultured at low densities or stimulated by TGF-β1 differentiate into myofibroblasts.[15,22]

In this study, we explore functional differences between fibroblasts and myofibroblasts in vitro, including extracellular matrix synthesis, activation of latent TGF-β after thrombin challenge, cellular migration, and proliferation. We use a novel technique to visualize, isolate, and manipulate keratocytes by taking advantage of their unique expression of keratocan.

Materials and Methods

A Novel Transgenic Mouse Strain to Trace Keratocyte-Derived Cells

An inducible *KeraRT/tetO-Cre* mouse model obtained from Professor C. Y. Liu's laboratory[23] was bred with the *Rosa26*^{mTmG} mouse (Stock 008463, Jackson Labs, Bar Harbor, ME, USA). They generated a triple transgenic conditional *KeraRT/tetO-Cre/mTmG* mouse strain, which contains both a Cre recombinase system and a Tet-On system associated with the keratocan gene. When these mice are fed doxycycline-containing diets, transmembrane tandem dimer Tomato (tdTomato) is knocked out and replaced with enhanced green fluorescent protein (eGFP) exclusively in keratocan-expressing cells. These cells continue to express eGFP even after differentiation. Cells that do not express keratocan at the time of induction continue to express tdTomato. In this paper, we will use *I-KeramTmG* to denote mice that have been induced to express eGFP.

Creation of a Full-Thickness Keratotomy for Evaluation of Scar Matrix and Cells

All experiments conformed to the use of Laboratory Animals and ARVO statement for the Use of Animals in Ophthalmic and Vision Research and were approved by the Institutional Animal Care and Use Committee of the University of South Florida College of Medicine. For injury experiments, adult, 60-day-old male mice were anesthetized, and subcutaneous analgesia was administered. Once the mouse was under general anesthesia, 0.1 mL of 0.5% proparacaine hydrochloride and atropine 1% was added to the ocular surface. Under microscope visualization, a full-thickness corneal incision, 1 mm in length, was made centrally in the cornea with a 15-degree blade. Immediately after the procedure, drops of moxifloxacin and artificial tear ointment were applied to the ocular surface. Mice were housed and treated in accordance with National Institutes of Health's (NIH's) Guide for the Care and Use of Laboratory Animals. Eyes were enucleated 12 weeks after injury for examination of scar cell phenotype. *I-KeramTmG* mice were fed doxycycline-supplemented diet for 1 week prior to enucleation.

Isolation and Culture of Fibroblasts and Induction of Myofibroblast Conversion

To obtain a pure expanded population of keratocyte-derived fibroblasts, we used our *I-KeramTmG* model. After euthanasia at 60 days of age, the eyes of adult *I-KeramTmG* mice were enucleated and washed twice with betadine ophthalmic solution (Alcon, Fort Worth, TX, USA). Eyes were incubated in DMEM containing 15 mg/mL dispase II (Roche Applied Science) at 4°C for 18 hours. The entire corneal epithelium could then be removed by vigorous shaking. Under a dissecting microscope, the corneal stroma was separated from sclera at the limbus by pressing down the corneoscleral junction with a 27-gauge needle.[13] Isolated corneal stromas were incubated overnight at 37°C in DMEM containing 1.25 mg/mL collagenase A (Roche Applied Science, Penzberg, Germany) and 25 µg/mL gentamicin. A keratocyte-containing cell suspension was then seeded on T25 flasks (Thermo Fischer Scientific, Waltham, MA, USA) in DMEM containing ITS (5 µg/mL insulin, 5 µg/mL transferrin, and 10 ng/mL sodium selenite), and 25 µg/mL gentamicin supplemented with 5% FBS. The suspension of stromal cells obtained from 6 mouse corneal buttons was poured into T25 flasks or glass slides for imaging. Stromal cells were then cultured on DMEM containing ITS and 5% FBS (fibroblast culture media). Once the cells attained confluency, a second group (myofibroblast) received additional 10 ng/mL of TGF-β1 in DMEM containing ITS and 1% FBS.

Flow Cytometry and Cell Sorting

Keratocyte-derived fibroblasts from *I-KeramTmG* mice were sorted via flow cytometry. After cells were cultured and expanded until confluence, single cell suspension was obtained by trypsinization, washed with Dulbecco's phosphate-buffered saline (DPBS) plus 25 mM HEPES,

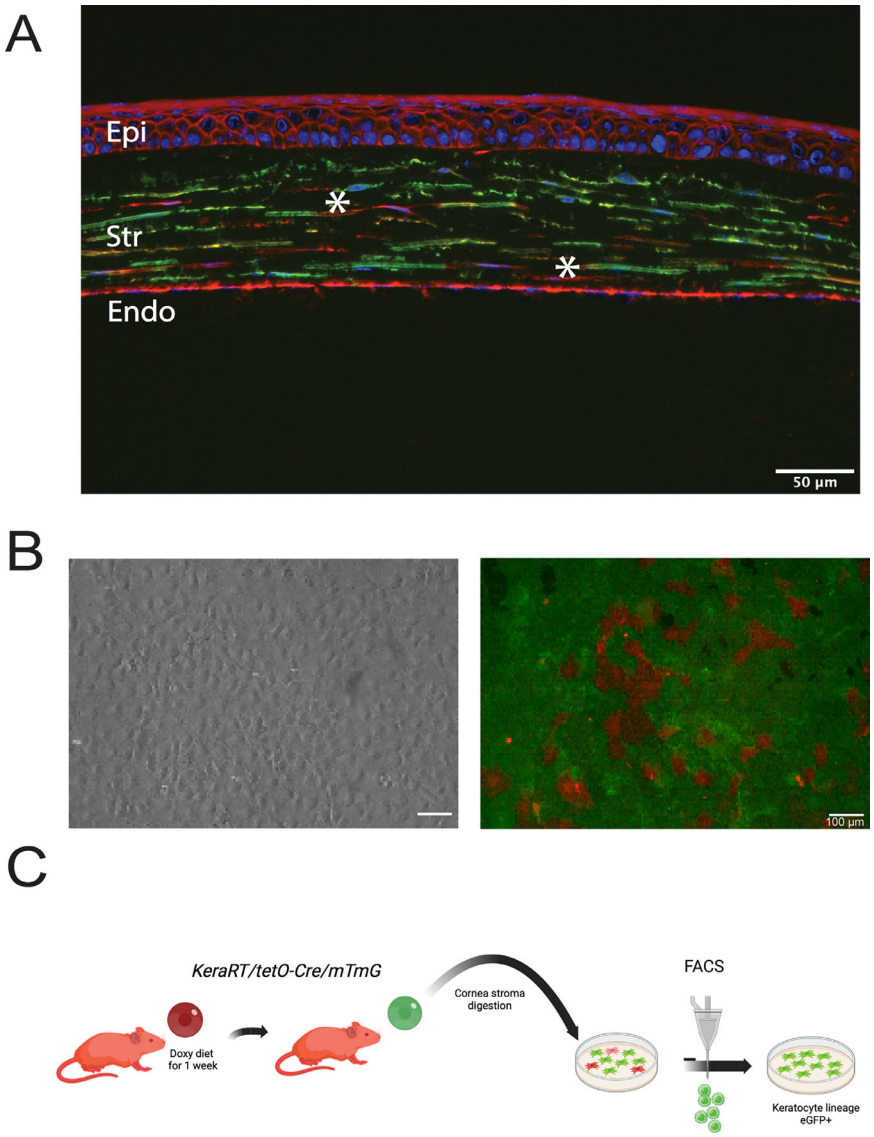

Figure 1. An inducible triple transgenic conditional *KeraRT/tetO-Cre/mTmG* mouse allows induction of eGFP expression in vivo by keratocytes after doxycycline-containing diet. (**A**) Most stromal cells (uninjured cornea) express eGFP (*green*) after 1 week of oral doxycycline supplementation. The eGFP+ and *orange* cells are believed to be keratocytes or derived from keratocytes. Some sparse cells in the stroma do not express keratocan and maintain tomato expression, marked by *asterisks*. (**B**) Phase contrast (*left*) and fluorescence (*right*) microscopy images of expanded corneal fibroblasts showing a mostly homogeneous population of cells, except for interspersed clusters of tdTomato-expressing cells (*red*). (**C**) Using flow cytometry, a pure sample of eGFP+ cells can be obtained from cultured fibroblasts. This purified sample consists only of cells derived from a keratocyte lineage. Epi, epithelium; Str, stroma; Endo, endothelium; FACS, fluorescence-activated cell sorting.

suspended into the same DPBS/HEPES buffer plus 1% dialyzed FBS, then transferred into a 5 mL polypropylene FACS tube with a cell strainer filter cap. Sorting of the eGFP positive cells was done on a Becton Dickinson (San Jose, CA, USA) FacsMelody with a 100 mM nozzle, using FACSChorus software. The eGFP positive single cells were identified by using no-eGFP matching cells as negative control. The brightest 30% of the positive cells were sorted with NERL Diluent 2 (Thermo Scientific, Waltham, MA, USA) as sheet fluid. After sorting, the cells were immediately pelleted and resuspended in growth media. The eGFP positive cells selected after flow cytometry were expanded with fibroblast culture medium (Fig. 1B). To induce myofibroblast conversion, confluent fibroblasts were placed in DMEM containing ITS and 1% FBS and supplemented with 10 ng/mL human recombinant TGF-β1 (Sigma Aldrich, St. Louis, MO, USA).

RNA Isolation and Quantification of mRNA

Total RNA was extracted using QIAzol Lysis Reagent (Qiagen, Hilden, Germany) and RNeasy MinElute Cleanup Kit (Qiagen) from expanded fibroblasts and myofibroblasts. Reverse transcription and quantitative real-time PCR analysis were performed as previously described.[24,25] See the Table for primer sequences used. Each sample was run in duplicate PCRs. Isolation and measurements were repeated three times.

Investigative Ophthalmology & Visual Science

Table. Primers Used in This Paper.

Gene	Forward Primer	Reverse Primer
Serpine-1	5′-GTCTTTCCGACCAAGAGCAG-3′	5′-GACAAAGGCTGTGGAGGAAG-3′
Col1a1	5′-TTCTCCTGGCAAAGACGGACTCAA-3′	5′-AGGAAGCTGAAGTCATAACCGCCA-3′
Col5a1	5′-AAGCGTGGGAAACTGCTCTCCTAT-3′	5′-AGCAGTTGTAGGTGACGTTCTGGT-3′
Col3a1	5′-CACGCAAGGCAATGAGACTA-3′	5′-TGGGGTTTCAGAGAGTTTGG-3′
Acta2	5′-AGATGACCCAGATCATGTTTGAGA-3′	5′-CACAGCCTGGATGGCTACGT-3′
Ltbp1	5′-ATGGATTCCAGCTGAACGAC-3′	5′-ACTCCCCATGAGATCCACAG-3′

Mass Spectrometry and Proteomics Analysis

To analyze differences in the expression of major matrix components between expanded fibroblasts and myofibroblasts derived from a keratocyte lineage, protein extracts obtained from confluent T25 flasks at first passage were analyzed from 3 different sets of cultures in each condition. Six to 10 corneas in each flask were used for primary culture that were later selected for eGFP selection with flow cytometry.

Proteomic Analysis

STRAP Protein Digestion. In brief, protein extracted from expanded fibroblasts and myofibroblasts was lysed in 50 mmol/L triethylammonium bicarbonate buffer, pH 7.55, containing 5% SDS. To ensure no DNA remained to prevent the trap from clogging, the solution was then sheered thoroughly by probe sonication at 20% amplitude, 5 seconds on and 5 seconds off, for 30 seconds. An S-Trap micro column (Protifi, Farmingdale, NY, USA) was placed in a 1.7-mL tube to retain flow-through. The sample mixture was then added into the micro column 200 µL at a time, followed by centrifugation of the micro column at 4000 × *g* for 1 minute. The flow-through was removed and the process repeated until the entire sample had passed through the S-Trap. The S-Trap micro column was then capped to limit evaporative loss without forming an airtight seal and incubated in a heat block for 37°C overnight. After digestion, peptides were eluted with 40 µL of 50 mmol/L triethylammonium bicarbonate and centrifugation at 4000 × *g* for 1 minute. Peptides were characterized using a Thermo Q-Exactive-HF mass spectrometer (Thermo Fisher Scientific) coupled to a Thermo Easy nLC 1200 (Thermo Fisher Scientific). The mass spectrometer was outfitted with a Thermo Nanospray Flex source (Thermo Fisher Scientific) with the following parameters: spray voltage = 2.24; capillary temperature = 225°C; and funnel RF level = 40. After protein identification, peptides for parallel reaction monitoring screening were chosen, the maximum time allowed for the instrument to acquire each specific ion was increased to 150 milliseconds, and the loop count was modified for the number of peptide masses chosen. Experiments were done in triplicates.

Confirmation of Collagen Expression by Wes Protein Analysis

To examine differences in the expression of relevant collagens (e.g. collagens I and V, fibril-forming collagens) and to confirm mass spectrometry data, protein extracts obtained from expanded fibroblasts and myofibroblasts were analyzed. Protein extraction was done using radioimmunoprecipitation assay (RIPA) lysis buffer. Protein concentration was determined through a bicinchoninic acid assay (BCA; Thermo Scientific Pierce). Expression of collagens I and V was analyzed using Wes Simple Western System (ProteinSimple, San Jose, CA, USA) following the manufacturer's instructions. The 12-230 kDa separation module anti-rabbit detection module was used. Briefly, samples diluted with 0.1 X sample buffer (ProteinSimple) at concentrations of 0.5 µg/µL were loaded and hybridized with anti-mouse collagen I (Sigma-Aldrich), anti α-smooth muscle actin (Abcam, Cambridge, UK), and rabbit anti collagen V antibodies[26] (1:100 dilution). Actin (Sigma-Aldrich) was used as a loading control. Experiments were done in triplicates.

Immunofluorescence

Expanded fibroblasts were seeded into glass slides for immunostaining. Myofibroblast induction was achieved by culture in 1% FBS in DMEM with 10 ng/mL TGF-β for 5 to 7 days. Fibroblasts were maintained in 5% FBS in DMEM for the same time period. Fibroblasts and myofibroblasts were fixed in 4% paraformaldehyde for 20 minutes, followed by blocking in 10% donkey serum for 30 minutes to 1 hour, and then incubation with primary antibody overnight at 4°C. Cells were then incubated in secondary antibody for 1 to 2 hours at room temperature. Slides were washed with 1 X PBS three times between each step. Primary antibodies and concentrations used for immunocytochemistry: anti-fibronectin EDA (1:400; Novus Biologicals NBP1-91258), anti-alpha smooth muscle actin 1A4 (1:100; Invitrogen 14976082), anti-LTBP1 (1:100; Sigma-Aldrich ABS504).

TGF-β Activation by Keratocyte-Derived Fibroblasts and Myofibroblasts After Thrombin Stimulation

Expanded fibroblasts and myofibroblasts were stimulated with 0.5 u/mL thrombin (Sigma-Aldrich) for 1 hour in serum free medium to stimulate cell contraction and assess the activation of latent TGF-β in the fibroblast or myofibroblast matrix.[27] The collected medium, including TGF-β, released by fibroblasts and myofibroblasts was then used to stimulate our TGF-β reporter cell system, as described previously.[28] Briefly, transformed mink lung cells transfected with luciferase cDNA driven by plasminogen activator inhibitor (PAI-1) promoter (a generous gift of Dr. Daniel Rifkin, New York University, New York, NY) were seeded and allowed to attach to a 24-well plate for 3 to 4 hours. Media from fibroblasts or myofibroblasts cultures was placed into individual wells within the 24-well plate. Then, 10 µmol/L TGF-β type I receptor/activin receptor-like kinase 5 (ALK5) inhibitor, SB431542 (Tocris Bioscience, Minneapolis, MN, USA) was used as a negative control. Luciferase assay was performed by using Promega's Luciferase Assay System (Promega, Madison, WI, USA), and luminescence

Investigative Ophthalmology & Visual Science

was measured with a Synergy HT microplate reader (BioTek Instruments, Winooski, VT, USA). Experiments were done in triplicates.

Wound Healing Assay

An in vitro wound healing assay was used to assess the migration and wound healing capabilities of keratocyte-derived fibroblasts and myofibroblasts. A linear scratch wound was induced in each well using a 1 mL sterile pipette tip. The cells were washed gently with DMEM and culture media were replaced with the appropriate medium for each group. Phase contrast and fluorescence images were obtained for each wound immediately after creation and at 12, 24, 48, and 90 hours. Images were analyzed using ImageJ software (National Institutes of Health, Bethesda, MD, USA) with the MRI Wound Healing tool (https://github.com/MontpellierRessourcesImagerie/imagej_macros_and_scripts/wiki/) for automated measurement of wound area. The experiment was repeated one additional time for confirmation of results. Experiments were done in triplicates.

Transwell Migration Assay

A transwell migration assay was performed to assess the invasion and chemotaxis ability of keratocyte-derived fibroblasts and myofibroblasts. After flow cytometry and cell sorting, eGFP-positive fibroblasts from *I-KeramTmG* mice were grown to confluence in two groups. After conversion of fibroblasts to myofibroblasts, both groups of cells were detached by trypsinization and seeded onto cell culture inserts with 8-µm pores preloaded into a 24-well plate (Nunc Polycarbonate Cell Culture Inserts; Thermo Scientific). Cell culture media was added to each well underneath the insert to establish a chemotactic gradient; 5% FBS in DMEM was used for fibroblasts, and 1% FBS in DMEM with 10 ng/mL TGF-β1 was used for myofibroblasts. The cells were incubated at 37°C for 24 hours, then, the inserts were removed and incubated in 4% paraformaldehyde for fixation of the migrated cells. The membranes were mounted upside-down on glass slides and stained with DAPI. Images were obtained and cells counted automatically using ImageJ software.

Cell Proliferation Assay

To compare the proliferation of fibroblasts and myofibroblasts, an MTT assay was performed. Corneal fibroblasts, derived from keratocytes isolated from *I-KeramTmG* mice, were seeded into a tissue culture-treated 96-well plate at a density of 3×10^3 cells/well. After cell monolayers reached confluence, half of the cells were maintained in 5% FBS in DMEM (fibroblasts) whereas the other half was switched to 1% FBS in DMEM supplemented with 10 ng/mL TGF-β1 (myofibroblasts). Pre-mixed MTT and solubilization buffer were added at manufacturer-specified concentrations and time points (Roche Cell Proliferation Assay I; Sigma Aldrich). Absorbance was measured at 575 nm and additionally at a reference wavelength of 700 nm using a Synergy HT microplate reader (BioTek Instruments, Winooski, VT, USA). Wells containing only culture media and no cells were used as blanks to control for background absorbance. Experiments were done in duplicates.

Statistical Analysis

GraphPad Prism version 9.1.2 (San Diego, CA, USA) was used for all statistical analyses and data are shown as means ± standard deviation. Statistical significance between two conditions was evaluated by the unpaired two tailed Student *t*-test. Statistical significance in experiments with more than two conditions (e.g. luciferase assay) was evaluated by 1-way ANOVA with the post hoc Holm-Šídák test to adjust for multiple comparisons. Wound healing assay results were analyzed using 2-way mixed ANOVA with the post hoc Šídák test. Values with $P < 0.05$ were considered statistically significant (*$P < 0.05$; **$P < 0.01$; ***$P < 0.005$; and ****$P < 0.001$).

Results

A *KeraRT/tetO-Cre/mTmG* Mouse Model can be Used to Isolate Keratocyte-Derived Cells

To further study the function of fibroblasts and myofibroblasts, and stromal cells known to regulate scar formation in the cornea, we used our *I-KeramTmG* mouse model to ensure that they originated from corneal keratocytes. As discussed above, in our mouse model, doxycycline supplementation induces the expression of eGFP exclusively in cells where the keratocan promoter is active. Histology sections show a high percentage of cells in uninjured *I-KeramTmG* stromas express eGFP after 1 week of doxycycline supplementation as most cells are expected to be keratocytes. A small number of stromal cells did not express eGFP and thus exhibited red fluorescence (asterisks in Fig. 1A). Epithelial and endothelial cells expressed tdTomato. Expanded corneal fibroblasts contain tdTomato clusters despite being induced in vivo before isolation (see Fig. 1B). These clusters can be sorted out by fluorescent activated cell sorting (FACS), ensuring the generation of a homogeneous population of eGFP-positive keratocyte-derived cells (Fig. 1C).

Corneal Scars are Characterized by Disorganized Cells and Deposited Collagen

We used second harmonic generation (SHG) imaging to evaluate the cellular and matrix organization in mature scars, formed 12 weeks after injury ($n = 6$). For comparison between normal uninjured stromas and scars, we imaged the contralateral uninjured central corneal stroma in our mouse models. In uninjured stromas, we found flat keratocyte bodies with their cell processes well aligned and parallel between lamellae (Figs. 2B, 2D). A distinct pattern of well-organized lamellae and collagen structures that were aligned in parallel with the epithelium and Descemet's membrane were evident (seen in gray in Fig. 2B). In contrast, imaging of stromal scars created by our injury model (Fig. 2E) showed a disorganized array of stromal cells that varied in morphology and did not maintain spacing and parallelism (Figs. 2G, 2H). Similarly, matrix collagen fibrils were deposited in a disorganized pattern without distinct lamellar structures, demonstrating that corneal scarring following injury is characterized by deposition of collagen fibrils (among other matrix components) in a disorganized fashion (Figs. 2F–H). These findings show that poor cell organization and disorganized matrix are hallmarks of corneal scars. Interestingly, corneal scars are characterized by an absence of keratocytes up to 12 weeks after injury, as evidenced by the lack of

Investigative Ophthalmology & Visual Science

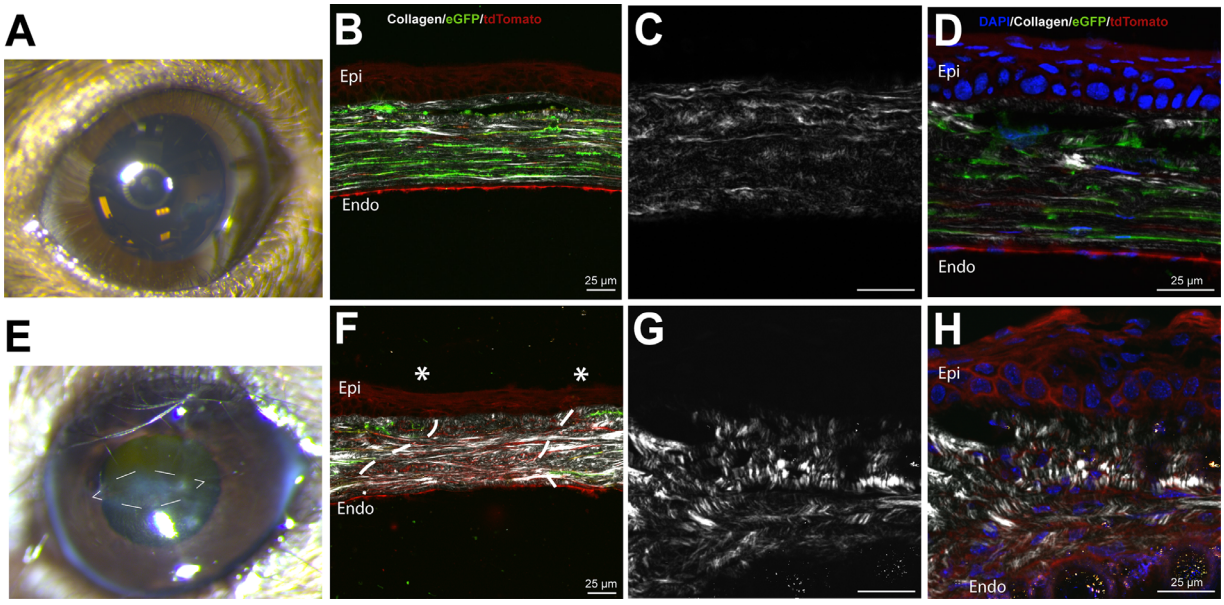

Figure 2. Corneal scars are composed of disorganized extracellular matrix and non-keratocyte cellular components. SHG microscopy was used for high-magnification imaging of collagen organization in mature corneal scars and uninjured corneas. (**A**) One of the most important properties of a normal cornea is transparency. (**B**) In an uninjured cornea, keratocytes (eGFP+) are well organized and located in a parallel orientation between the corneal lamellae. Keratocytes make up most cells in the normal uninjured stroma. (**C**) Higher-magnification image of collagen fibrils in a normal cornea. (**D**) High-magnification image of a normal mouse cornea including nuclear counterstain. Keratocytes (eGFP+) is predominant population. (**E**) Cornea with central scar (*dashed outline*), imaged 9 weeks after full-thickness keratotomy. (**F**) Within the area of the scar (*dashed lines*), there is lack of eGFP expression in response to doxycycline induction meaning keratocytes do not populate scars. *Asterisks* mark limit between keratocytes (eGFP+) and fibroblasts (Tdtomato+) populations. Distinct lamellae are largely absent and collagen matrix is very disorganized in comparison to normal cornea in scars. (**G, H**) High-magnification images of corneal scar, again showing disorganization of the collagen matrix and the absence of eGFP+ keratocytes. Epi, epithelium; Endo, endothelium.

eGFP-expressing cells in the scar after 1 week of doxycycline induction (see Figs. 2F, 2H).

Fibroblasts and Myofibroblasts Derive From a Keratocyte Lineage

As expected, there were significant morphological differences between fibroblasts and myofibroblasts derived from a keratocyte lineage after 1 week in culture with different medium conditions, including exposure to TGF-β1. Expanded fibroblasts cultured in serum-free DMEM had a larger cytoplasm and flat appearance. Fibroblasts expanded in DMEM medium supplemented with 5% FBS were smaller and had a higher proliferative cell density. Fibroblasts maintained a broad cytoplasmic contour. In contrast, myofibroblasts, exposed to TGF-β1 for 1 week, were more spindled shaped with disorganized cell-cell relationships (Fig. 3A). These findings corroborate the significant influence of TGF-β1 in regulating the morphology of a keratocyte lineage and demonstrate that stromal fibroblasts and myofibroblasts unequivocally derive from a keratocyte lineage.

Myofibroblast Conversion Comes With Downregulation of Collagens I and V Expression

To quantify and compare the expression of different extracellular matrix components in fibroblasts and myofibroblasts, we first used quantitative real-time PCR (qRT-PCR) to assess several genes of known importance during wound healing. Expression of PAI-1 and αSMA was upregulated in cells stimulated with TGF-β1, confirming their conversion to myofibroblasts. Fibroblasts upregulated different matrix components in comparison to myofibroblasts. Higher expression of collagens I and V, the main components of corneal collagen fibrils, was noted in keratocyte-derived fibroblasts when compared to myofibroblasts. Expression of latent TGF-β-binding protein 1 (LTBP-1), a known regulator of latent TGF- β activation, was increased in fibroblasts compared to myofibroblasts (Fig. 3B).

Fibroblast and Myofibroblast Deposit a Significantly Different Matrix In Vitro

To compare the extracellular matrices created by fibroblasts and myofibroblasts, we quantified the expression of different matrix components and imaged the deposition of collagen fibrils by fibroblasts and myofibroblasts in vitro after 1 week in culture. Proteomic analysis of individual collagen chains and other relevant matrix components revealed significant differences in extracellular matrix composition between fibroblasts and myofibroblasts. Contrary to our expected findings, and consistent with gene expression data, deposition of collagens I and V (the main corneal collagen fibril components) was decreased in the myofibroblast matrix (Fig. 4A). This finding was additionally confirmed by Western blot analysis (Fig. 4B). Collagens VI and XIV were also downregulated in this group. Fibrillin, syndecan-1, fibronectin, and biglycan were upregulated in the myofibroblast matrix (see Fig. 4A).

Second harmonic generation imaging shows differences in the patterns of matrix deposition between fibroblasts and myofibroblasts. Fibroblasts appear to deposit collagen fibrils

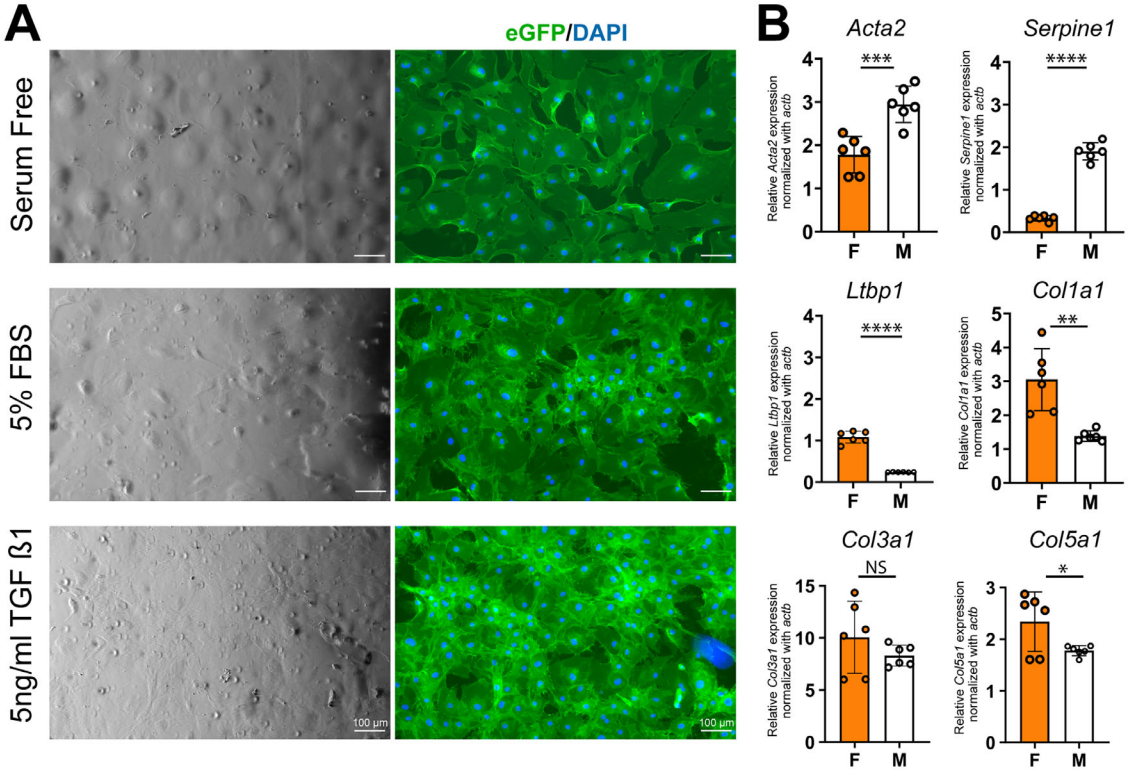

Figure 3. Morphological and matrix expression differences between keratocyte derived fibroblasts and myofibroblasts in vitro. (**A**) Corneal fibroblasts were cultured in DMEM (*top*), 5% FBS in DMEM (*middle*), and 5% FBS in DMEM supplemented with 10 ng/mL TGF β1 (*bottom*). Images shown were obtained by phase contrast (*left column*) and fluorescence (*right column*) microscopy. Changes in cellular morphology are evident with different culture conditions, reflecting cellular activity and differentiation. (**B**) Quantitative RT-PCR shows differences in gene expression between keratocyte-derived fibroblasts and myofibroblasts. Specifically, myofibroblasts showed significantly greater expression of *Acta2* and *Serpine1* and less expression of *Ltbp*, *Col1a1*, and *Col5a1* when compared with fibroblasts. No significant difference in *Col3a1* expression was found. F, fibroblast; M, myofibroblast; NS, not significant. *:$P < 0.05$; **: $P < 0.01$; ***: $P < 0.005$; ****: $P < 0.001$. Scale bars = 100 µm.

in their pericellular space in a regular pattern, in contrast to the more disorganized and irregular matrix of myofibroblasts (Fig. 4C). The myofibroblast matrix is characterized by areas of dense collagen deposition and variable fibril orientation. Immunostaining for fibronectin extra domain A, an alternative splicing variant of fibronectin, reveals that it appears to be upregulated by myofibroblasts (Fig. 5A). These findings show that the extracellular matrices of fibroblasts and myofibroblasts differ in both composition (of collagen and non-collagen components) and organization.

Corneal Fibroblasts Cannot Activate Latent TGF-β From Their Matrix

The expression of αSMA in myofibroblasts bestows these cells with contractile properties. To assess the contractile properties of these cells in vitro and their effectiveness in activating latent TGF-β deposited in the matrix, we allowed fibroblasts and myofibroblasts to deposit extracellular matrix for 1 week and then stimulated contraction with a low dose of thrombin.[27] We assume that fibroblasts and myofibroblasts deposit similar amounts of latent TGF-β, because no obvious difference in LTBP1 content was noted by mass spectrometry in both cell types (see Fig. 4A). Fibroblasts exhibited low levels of active TGF-β release, similar to controls, and this did not increase significantly with the addition of thrombin. In contrast, myofibroblasts consistently activated latent TGF-β deposits and were stimulated to increase this activation upon thrombin-mediated contraction (Fig. 6A). These findings demonstrate that corneal myofibroblasts are potent activators of latent TGF-β, whereas fibroblasts are not.

Fibroblasts and Myofibroblasts Differ in Proliferation and Chemotaxis Abilities

Wound healing and transwell migration assays were performed to compare the migratory and chemotactic capabilities of fibroblasts and myofibroblasts. Cell type was not found to have a significant impact on wound closure over time ($P > 0.05$). At each time point, fibroblasts and myofibroblasts had similar percentages and rates of wound closure (Fig. 7A). When chemotaxis was assessed by transwell migration, a significantly greater quantity of fibroblasts had migrated at 24 hours when compared to myofibroblasts ($P < 0.05$; Fig. 7B). Fibroblasts also demonstrated significantly greater metabolic activity than myofibroblasts when assessed by MTT assay ($P < 0.05$; Fig. 7C), which suggest greater proliferation.

Investigative Ophthalmology & Visual Science

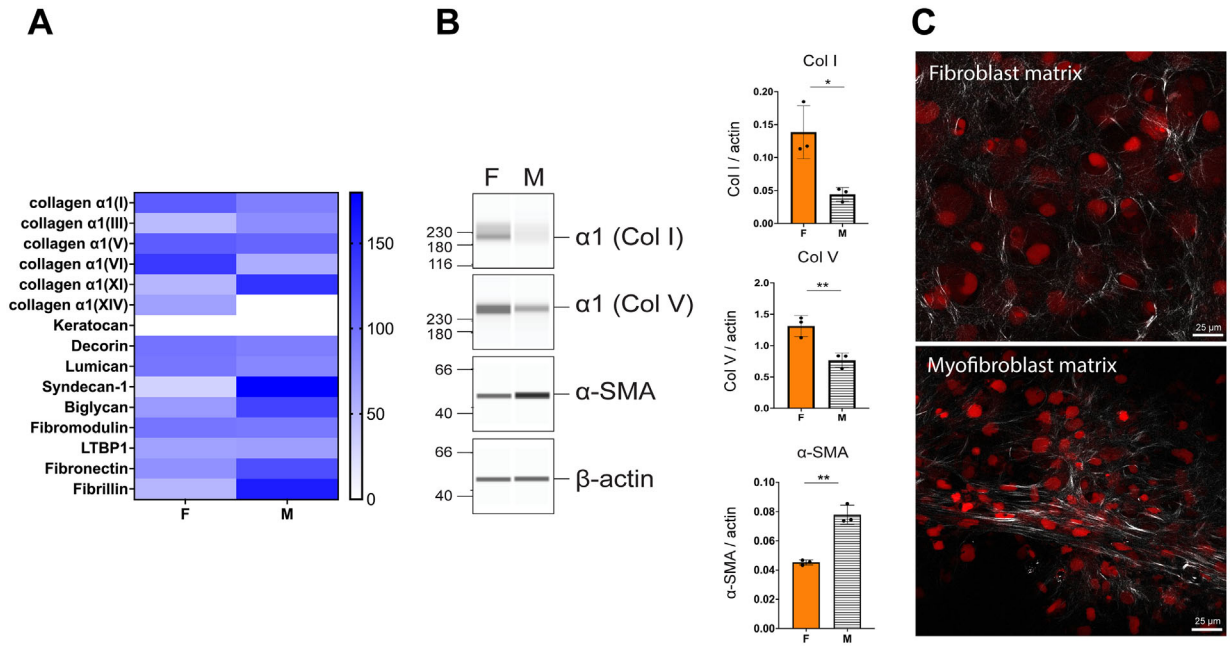

Figure 4. Protein analysis confirms higher deposition of most collagens in the "fibroblast matrix" compared to a "myofibroblast matrix". (**A**) Heat map of proteomic analysis data comparing the quantities of extracellular matrix proteins deposited by fibroblasts and myofibroblasts. Fibroblasts had higher quantities of most collagens, whereas other non-collagen components were upregulated by myofibroblasts. (**B**) Western blot confirms that fibroblast matrix contains significantly higher quantities of collagen I and collagen V α1 chains. As expected, myofibroblasts contain significantly higher quantities of αSMA, an important marker of the myofibroblast phenotype. Results were normalized using β-actin. F, fibroblast; M, myofibroblast. *: $P < 0.05$; **: $P < 0.01$. (**C**) Visualization of in vitro fibroblast and myofibroblast extracellular matrix deposition using SHG microscopy. Note how collagen structures are deposited in a more disorganized pattern by myofibroblasts compared to fibroblasts. Nuclei are highlighted in *red* due to staining with propidium iodide.

Discussion

During the process of corneal wound healing, keratocytes differentiate to fibroblasts and myofibroblasts to occupy and rapidly heal injuries and close tissue defects by depositing extracellular matrix.[29] Prompt closure of corneal wounds is essential to avoid the loss of intraocular contents, prevent infection, and regain tissue function.[7,12] However, this initial tissue response often evolves to formation of scar tissue of significant severity and impairs tissue function.

It is unknown if fibroblasts and myofibroblasts originate exclusively from keratocytes or if they could be derived from other cells, such as immune cells, Schwann cells, or circulating blood-derived cells homing to the corneal stroma during inflammation and injury.[7,12,30] In other tissues and organs, cell lineage tracing models have shown that myofibroblasts can originate from local quiescent fibroblasts in addition to pericytes, mesenchymal stem cells, vascular endothelial cells via endothelial-mesenchymal transition, epithelial cells via epithelial-mesenchymal transition, and bone marrow-derived circulating fibrocytes.[10] In the cornea, fibrocytes and bone marrow-derived cells are known to home in the stroma after bone marrow transplantation, and it is believed that they contribute to the wound healing process with some cells transforming to myofibroblasts.[31] Using our novel mouse strain that allows lineage tracing by expression of eGFP, we can directly demonstrate that keratocytes give rise to fibroblasts and myofibroblasts. Our mouse model does not exclude the possibility that some myofibroblasts in scars could originate from bone marrow cells or other sources and future in vivo studies are needed to answer this question.

Our SHG data show how crucial organization of stromal cells and collagen fibril deposition is in the formation of corneal scarring. Evaluation of mature scars, 12 weeks after trauma, in our injury model clearly shows loss of cellular organization with increased number of stromal cells with lost cell polarity. Similarly, significant disorganization is seen in the deposited extracellular matrix following repair of tissue injury. The interwoven, rather than parallel, pattern of collagen fibril deposition has been hypothesized to give the fibrotic tissue the requisite strength and rigidity to support the remodeling of damaged normal stroma.[32] More investigations are needed to better understand the molecular and mechanical mechanisms directing tissue repair after injury, especially those involved in fibrotic tissue remodeling and resolution.

Understanding corneal myofibroblast biology is essential to comprehending wound repair.[7,12,30] Persistence of myofibroblasts in the repaired tissue is associated with fibrosis and subsequent compromise of tissue function and vision loss.[12,30] How fibroblasts and myofibroblasts function and how their fate is regulated by the extracellular matrix during the process of corneal wound healing is not fully understood. The extracellular matrix is a complex structure, and it is well established that it directs resident cells' function and differentiation.[33,34] The extracellular matrix composition is dynamic as it changes during tissue repair. These alterations provide specific chemical and physical cues to resident cells that direct wound healing.[34–36] The matrix regulates growth factor accessibility, availability, and signaling.[33,34,37] Many matrix proteins provide a pericellular substrate for presenting growth factors and sequester active and latent cytokines.[35] As the extracellular matrix composi-

Investigative Ophthalmology & Visual Science

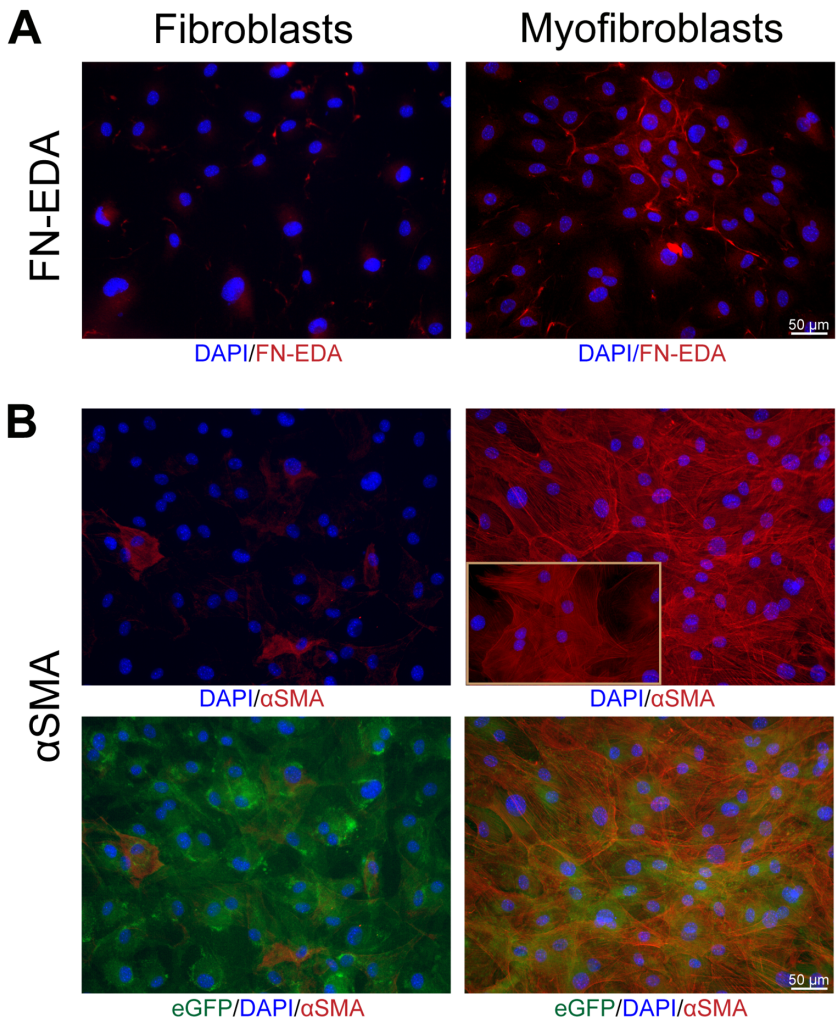

Figure 5. Differences in FN-EDA and αSMA expression between fibroblasts and myofibroblasts. (**A**) Fluorescence microscopy images of fibroblasts (*left*) and myofibroblasts (*right*) immunostained for fibronectin extra domain A (FN-EDA). Nuclei are counterstained with DAPI. (**B**) Fluorescence microscopy images of fibroblasts (*left*) and myofibroblasts (*right*) stained for alpha smooth muscle actin (αSMA). Nuclei are counterstained with DAPI. The inset image shows a higher-magnification view of αSMA-stained myofibroblasts. *Green* fluorescence in the bottom row of images is due to expression of eGFP by keratocyte-derived cells isolated from *I-KeramTmG* mice demonstrating these cells are derived from a keratocyte lineage.

tion changes during tissue repair, matrix-associated growth factors change in their availability and signaling, potentially affecting the function, differentiation, and survival of fibroblasts and myofibroblasts.[34] For example, it is known that myofibroblasts typically undergo apoptosis once the process of tissue repair is complete. This apoptosis is believed to be triggered by a rapid drop in tissue tension and depletion of trophic cytokines, of which TGF- β1 seems to be crucial.[38,39]

An unexpected finding is that fibroblasts secrete fibril-forming collagens in higher quantities than myofibroblasts, at least in vitro. This curious observation suggests that the association of myofibroblasts with fibrosis does not relate to increased synthesis of extracellular matrix (collagens) but to other functions of myofibroblasts, including mechanical contraction of the matrix with cytokine(s) activation, matrix cross-linking, or possibly disorganized accumulation of matrix components compared to fibroblasts. Our SHG data clearly show disorganized deposition of collagen fibrils in vitro by myofibroblasts. Such differences between fibroblasts and myofibroblasts in the expression and deposition of extracellular matrix likely play a vital role in regulating wound repair. The differences in the deposited extracellular matrix could ultimately regulate myofibroblast survival, which could be associated with extracellular matrix stiffness and other biomechanical properties. A stiffer matrix could facilitate the release of TGF-β, favoring conversion from fibroblasts to myofibroblasts. Once a significant number of fibroblasts become myofibroblasts, then myofibroblasts remodel the extracellular matrix and modify its mechanical properties, including the availability of cytokines. In this new myofibroblast-modified matrix, myofibroblasts cannot survive and undergo apoptosis, completing the process of wound healing (Fig. 8).

The results of cellular proliferation and migration studies also seem to support the above conclusions. Fibroblasts are thought to have greater proliferation and migration capabilities than myofibroblasts, which our study confirms. Fibroblasts are believed to be the first of the two to appear after injury and function to begin the process of extracellular

Investigative Ophthalmology & Visual Science

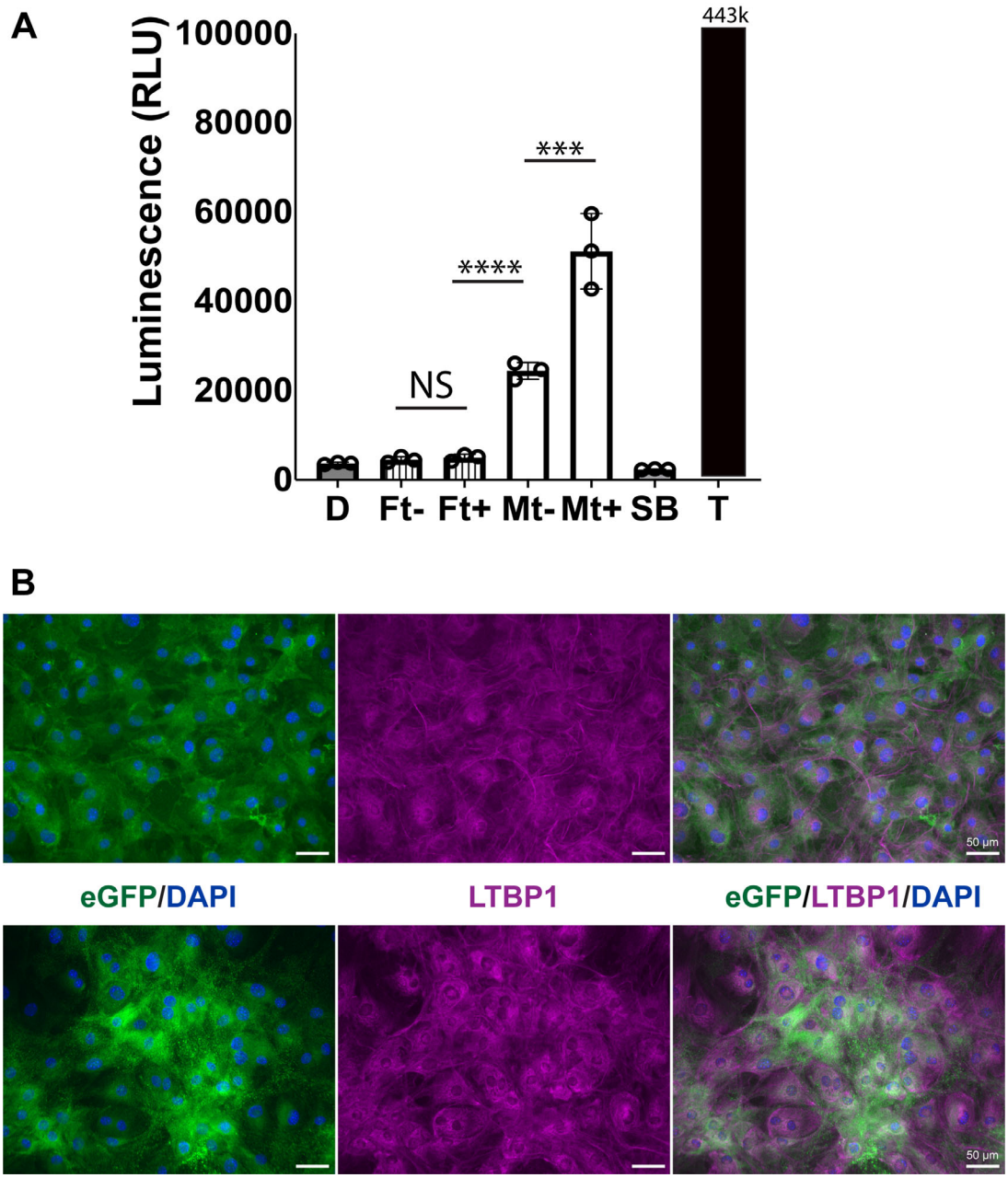

Figure 6. Myofibroblasts are more efficient in activating latent TGF- β from their matrix compared to fibroblasts after thrombin stimulation. This finding confirms that one of the main functions of myofibroblasts is cell contraction during wound closure. (**A**) Luciferase assay was used to quantify and compare the activation of latent TGF-β in fibroblasts and myofibroblasts. Higher luminescence (expressed as RLU) values indicate greater quantities of active TGF-β in the conditioned medium of cultured cells. Ft-, fibroblasts without thrombin; Ft+, fibroblasts with thrombin added; Mt-, myofibroblasts without thrombin; Mt+, myofibroblasts with thrombin added; D, DMEM only; SB, SB431542 (ALK inhibitor, negative control); T, TGF-β, positive control. (**B**) Fluorescence microscopy images of keratocyte-derived fibroblasts (*top row*) and myofibroblasts (*bottom row*) stained for LTBP1 (*purple*) and counterstained with DAPI (*blue*). These images show the deposition of LTBP1 in pericellular "strands" of extracellular matrix components by activated fibroblasts and myofibroblasts.

matrix deposition to fill the defect. Therefore, they should be able to sense and respond to changing concentrations of chemotactic growth factors to rapidly migrate to the site of injury, proliferate, and begin depositing new extracellular matrix. Myofibroblasts' major functions is the generation of force to bring wound edges together in the healing tissue. Therefore, proliferation and migration capabilities should be less important for myofibroblasts than they are for fibroblasts.

How TGF-β signaling, activation, and latency are regulated by the corneal stromal specific matrix (unique composition, hierarchical organization, and mechanics) after injury is unknown. TGF-β plays a major role in the corneal wound healing process.[7,40–43] TGF-β is regulated at multiple levels. A physical barrier for the action of TGF-β is the basement membrane.[44] An injured basement membrane allows entrance of TGF-β to the stroma and activation of fibroblasts and myofibroblasts.[44] During tissue repair after

Investigative Ophthalmology & Visual Science

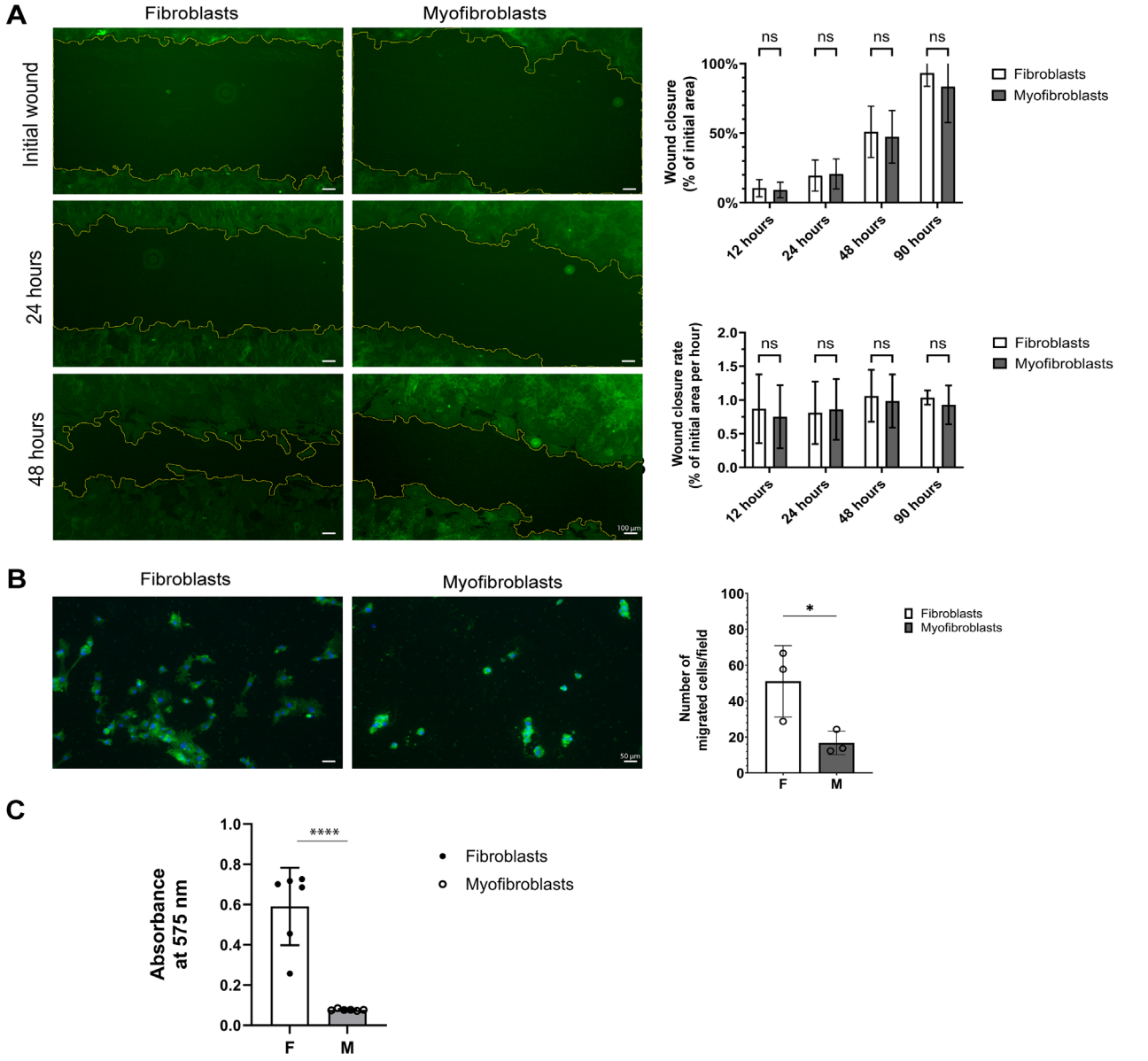

Figure 7. Results of wound healing, transwell migration, and MTT cell proliferation assays. (**A**) Fluorescence microscopy images of fibroblast (*left*) and myofibroblast (*right*) monolayers taken immediately, 24 hours, and 48 hours after creation of scratch wounds. Wound edges were outlined automatically in *yellow* by ImageJ software, which was used to measure wound area. The graphs represent data and comparisons for wound closure (*top*) and wound closure rate (*top*) at each time point. Wound closure is calculated as a percentage of the initial wound area, and wound closure rate is calculated as wound closure over time. (**B**) Results of transwell migration assay for fibroblasts and myofibroblasts. Images were taken of migrated fibroblasts (*left*) and myofibroblasts (*right*) on the undersides of transwell insert membranes after a 24-hour incubation period. The bars in the bar graph represent the average number of migrated cells per field for both cell types. (**C**) Bar graph representing MTT assay absorbance data for fibroblasts and myofibroblasts. Higher absorbance values indicate greater cell metabolic activity. F, fibroblasts; M, myofibroblasts; ns, no significant difference *: $P < 0.05$; ****: $P < 0.001$.

injury, a repaired and impermeable basement membrane is associated with myofibroblast apoptosis by preventing the entrance of TGF-β to the stroma. At the same time, stromal activity of TGF-β could be autoregulated by various extracellular matrix components like LTBPs, MAGPs, and fibrillin.[10,29,45] Fibronectin ED-A has also been found to promote TGF-β1 signaling and activation of myofibroblasts,[46] which explains why immunofluorescence was detected only in the myofibroblast matrix in our study. Similarly, depletion or poor activation of latent TGF-β stores might occur at the final stages of the wound healing process, inducing myofibroblast apoptosis or senesce.[29] Understanding the specific matrix components upregulated by myofibroblast is important because some of these matrix components could regulate myofibroblast transformation, survival, or fate.

A major limitation in this paper is the use of an in vitro system. The complexity of wound healing in vivo and the different stages of wound healing cannot be recreated in vitro. Our laboratory is currently expanding this work and

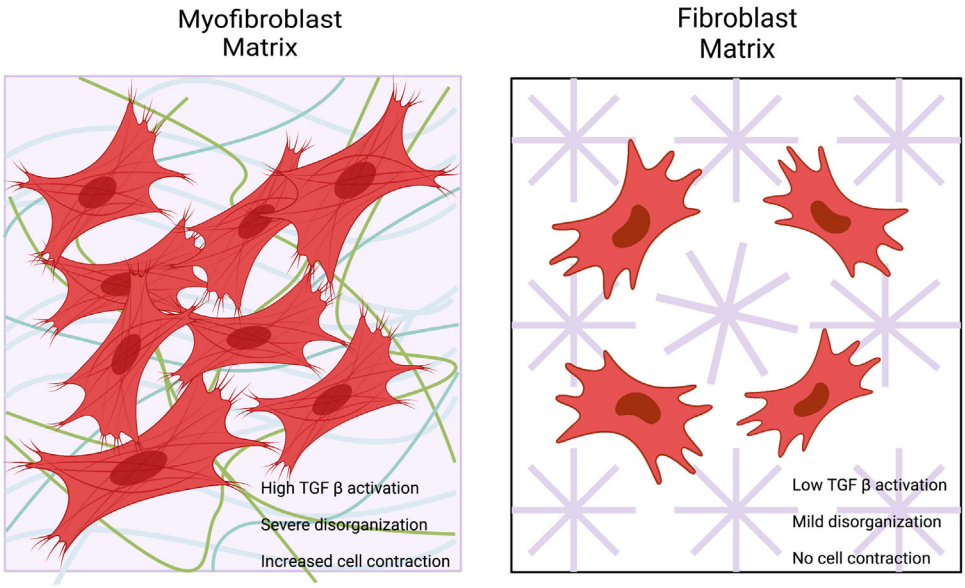

Figure 8. Illustration summarizing some of the main findings of this paper. Compared to fibroblasts, myofibroblasts are characterized by a higher propensity for TGFβ activation, deposition of disordered extracellular matrix (characterized in the figure by randomly oriented and shaped extracellular matrix strands, rather than uniform asterisk-like structures), and contraction of the cells and extracellular matrix. These key differences highlight the unique role of each cell type in physiologic and pathophysiologic processes of wound healing and scar formation.

evaluating lineage tracing and differences in cell phenotype during different stages of corneal wound healing in vivo. Another limitation is the heterogeneity of phenotypes within the fibroblast and myofibroblast populations.[29,47] However, our findings highlight the potentially significant differences in extracellular matrix expression by fibroblasts and myofibroblasts as well as functional differences, particularly in contracting tissue, organizing collagen fibrils in the matrix, and in activating latent TGF-β from the corneal matrix. Manipulation of fibroblast or myofibroblast matrix secretion or survival appear to be fertile avenues of investigation for the prevention and treatment of corneal scars.

Acknowledgments

The authors thank the USF Health Research Methodology and Biostatistics (RMB) Core for their assistance with data analysis.

Supported by NIH/NEI grants EY029395 and EY034114 and an unrestricted grant from the Department of Ophthalmology, University of South Florida, Tampa, FL, USA.

Author Contributions: Ana C. Acosta designed the research studies, analyzed the data, and wrote the manuscript; Hadi Joud conducted the experiments, acquired the data, analyzed the data, and wrote the manuscript; Mei Sun conducted the experiments, acquired the data, and analyzed the data; Curtis E. Margo analyzed the data, and wrote the manuscript; Marcel Y. Avila designed the research studies, analyzed the data, and wrote the manuscript; Edgar M. Espana designed the research studies, conducted the experiments, acquired the data, analyzed the data, and wrote the manuscript.

Disclosure: **A.C. Acosta**, None; **H. Joud**, None; **M. Sun**, None; **M.Y. Avila**, None; **C.E. Margo**, None; **E.M. Espana**, GSK (C)

References

1. Espana EM, Birk DE. Composition, structure and function of the corneal stroma. *Exp Eye Res*. 2020;198:108137.
2. Fini ME. Keratocyte and fibroblast phenotypes in the repairing cornea. *Prog Retin Eye Res*. 1999;18:529–551.
3. Poole CA, Brookes NH, Clover GM. Keratocyte networks visualised in the living cornea using vital dyes. *J Cell Sci*. 1993;106(Pt 2):685–691.
4. Yam GHF, Riau AK, Funderburgh ML, Mehta JS, Jhanji V. Keratocyte biology. *Exp Eye Res*. 2020;196:108062.
5. Liu CY, Birk DE, Hassell JR, Kane B, Kao WW. Keratocan-deficient mice display alterations in corneal structure. *J Biol Chem*. 2003;278:21672–21677.
6. Wilson SE. The corneal fibroblast: the Dr. Jekyll underappreciated overseer of the responses to stromal injury. *Ocul Surf*. 2023;29:53–62.
7. Wilson SE. Corneal wound healing. *Exp Eye Res*. 2020;197:108089.
8. Kamil S, Mohan RR. Corneal stromal wound healing: major regulators and therapeutic targets. *Ocul Surf*. 2021;19:290–306.
9. Hinz B, Lagares D. Evasion of apoptosis by myofibroblasts: a hallmark of fibrotic diseases. *Nat Rev Rheumatol*. 2020;16:11–31.
10. Hinz B. Myofibroblasts. *Exp Eye Res*. 2016;142:56–70.
11. Hinz B. The myofibroblast: paradigm for a mechanically active cell. *J Biomech*. 2010;43:146–155.
12. Wilson SE. Corneal myofibroblasts and fibrosis. *Exp Eye Res*. 2020;201:108272.
13. Kawakita T, Espana EM, He H, et al. Keratocan expression of murine keratocytes is maintained on amniotic membrane by down-regulating transforming growth factor-beta signaling. *J Biol Chem*. 2005;280:27085–27092.
14. Beales MP, Funderburgh JL, Jester JV, Hassell JR. Proteoglycan synthesis by bovine keratocytes and corneal fibroblasts:

maintenance of the keratocyte phenotype in culture. *Invest Ophthalmol Vis Sci*. 1999;40:1658–1663.
15. Jester JV, Barry-Lane PA, Cavanagh HD, Petroll WM. Induction of alpha-smooth muscle actin expression and myofibroblast transformation in cultured corneal keratocytes. *Cornea*. 1996;15:505–516.
16. Kawakita T, Espana EM, He H, et al. Preservation and expansion of the primate keratocyte phenotype by downregulating TGF-beta signaling in a low-calcium, serum-free medium. *Invest Ophthalmol Vis Sci*. 2006;47:1918–1927.
17. Espana EM, He H, Kawakita T, et al. Human keratocytes cultured on amniotic membrane stroma preserve morphology and express keratocan. *Invest Ophthalmol Vis Sci*. 2003;44:5136–5141.
18. Espana EM, Kawakita T, Di Pascuale MA, et al. The heterogeneous murine corneal stromal cell populations in vitro. *Invest Ophthalmol Vis Sci*. 2005;46:4528–4535.
19. Espana EM, Kawakita T, Liu CY, Tseng SC. CD-34 expression by cultured human keratocytes is downregulated during myofibroblast differentiation induced by TGF-beta1. *Invest Ophthalmol Vis Sci*. 2004;45:2985–2991.
20. Seidelmann N, Duarte Campos DF, Rohde M, et al. Human platelet lysate as a replacement for fetal bovine serum in human corneal stromal keratocyte and fibroblast culture. *J Cell Mol Med*. 2021;25:9647–9659.
21. Binte MYNZ, Riau AK, Yam GHF, Binte Halim NSH, Mehta JS. Isolation and propagation of human corneal stromal keratocytes for tissue engineering and cell therapy. *Cells-Basel*. 2022;11:1–18.
22. Masur SK, Dewal HS, Dinh TT, Erenburg I, Petridou S. Myofibroblasts differentiate from fibroblasts when plated at low density. *Proc Natl Acad Sci USA*. 1996;93:4219–4223.
23. Zhang Y, Kao WW, Hayashi Y, et al. Generation and characterization of a novel mouse line, keratocan-rtTA (KeraRT), for corneal stroma and tendon research. *Invest Ophthalmol Vis Sci*. 2017;58:4800–4808.
24. Sun M, Zafrullah N, Adams S, et al. Collagen XIV is an intrinsic regulator of corneal stromal structure and function. *Am J Pathol*. 2021;191(12):2184–2194.
25. Sun M, Zafrullah N, Devaux F, et al. Collagen XII is a regulator of corneal stroma structure and function. *Invest Ophthalmol Vis Sci*. 2020;61:61.
26. Sun M, Chen S, Adams SM, et al. Collagen V is a dominant regulator of collagen fibrillogenesis: dysfunctional regulation of structure and function in a corneal-stroma-specific Col5a1-null mouse model. *J Cell Sci*. 2011;124:4096–4105.
27. Wipff PJ, Rifkin DB, Meister JJ, Hinz B. Myofibroblast contraction activates latent TGF-beta1 from the extracellular matrix. *J Cell Biol*. 2007;179:1311–1323.
28. Sun M, Koudouna E, Cogswell D, Avila MY, Koch M, Espana EM. Collagen XII regulates corneal stromal structure by modulating transforming growth factor-beta activity. *Am J Pathol*. 2022;192:308–319.
29. Pakshir P, Noskovicova N, Lodyga M, et al. The myofibroblast at a glance. *J Cell Sci*. 2020;133:1–10.
30. Mohan RR, Kempuraj D, D'Souza S, Ghosh A. Corneal stromal repair and regeneration. *Prog Retin Eye Res*. 2022;91:101090.
31. Wilson SE, Sampaio LP, Shiju TM, Carlos de Oliveira R. Fibroblastic and bone marrow-derived cellularity in the corneal stroma. *Exp Eye Res*. 2021;202:108303.
32. Connon CJ, Meek KM. The structure and swelling of corneal scar tissue in penetrating full-thickness wounds. *Cornea*. 2004;23:165–171.
33. Rozario T, DeSimone DW. The extracellular matrix in development and morphogenesis: a dynamic view. *Dev Biol*. 2010;341:126–140.
34. Bonnans C, Chou J, Werb Z. Remodelling the extracellular matrix in development and disease. *Nat Rev Mol Cell Biol*. 2014;15:786–801.
35. Hynes RO, Naba A. Overview of the matrisome–an inventory of extracellular matrix constituents and functions. *Cold Spring Harb Perspect Biol*. 2012;4:a004903.
36. Humphrey JD, Dufresne ER, Schwartz MA. Mechanotransduction and extracellular matrix homeostasis. *Nat Rev Mol Cell Biol*. 2014;15:802–812.
37. Hynes RO. The extracellular matrix: not just pretty fibrils. *Science*. 2009;326:1216–1219.
38. Grinnell F, Zhu M, Carlson MA, Abrams JM. Release of mechanical tension triggers apoptosis of human fibroblasts in a model of regressing granulation tissue. *Exp Cell Res*. 1999;248:608–619.
39. Lodyga M, Hinz B. TGF-beta1 - A truly transforming growth factor in fibrosis and immunity. *Semin Cell Dev Biol*. 2020;101:123–139.
40. Wilson SE. TGF beta -1, -2 and -3 in the modulation of fibrosis in the cornea and other organs. *Exp Eye Res*. 2021;207:108594.
41. Tandon A, Tovey JC, Sharma A, Gupta R, Mohan RR. Role of transforming growth factor beta in corneal function, biology and pathology. *Curr Mol Med*. 2010;10:565–578.
42. Saikia P, Crabb JS, Dibbin LL, et al. Quantitative proteomic comparison of myofibroblasts derived from bone marrow and cornea. *Sci Rep*. 2020;10:16717.
43. McKay TB, Hutcheon AEK, Zieske JD. Biology of corneal fibrosis: soluble mediators, integrins, and extracellular vesicles. *Eye (Lond)*. 2020;34:271–278.
44. Wilson SE, Torricelli AAM, Marino GK. Corneal epithelial basement membrane: structure, function and regeneration. *Exp Eye Res*. 2020;194:108002.
45. Klingberg F, Hinz B, White ES. The myofibroblast matrix: implications for tissue repair and fibrosis. *J Pathol*. 2013;229:298–309.
46. Serini G, Bochaton-Piallat ML, Ropraz P, et al. The fibronectin domain ED-A is crucial for myofibroblastic phenotype induction by transforming growth factor-beta1. *J Cell Biol*. 1998;142:873–881.
47. Peyser R, MacDonnell S, Gao Y, et al. Defining the activated fibroblast population in lung fibrosis using single-cell sequencing. *Am J Respir Cell Mol Biol*. 2019;61:74–85.

Investigative Ophthalmology & Visual Science